LETTER

doi:10.1038/nature09646

Bifidobacteria can protect from enteropathogenic infection through production of acetate

Shinji Fukuda[1,2], Hidehiro Toh[3], Koji Hase[1], Kenshiro Oshima[4], Yumiko Nakanishi[1,2,5], Kazutoshi Yoshimura[6], Toru Tobe[7], Julie M. Clarke[8], David L. Topping[8], Tohru Suzuki[9], Todd D. Taylor[3], Kikuji Itoh[6], Jun Kikuchi[2,5,10], Hidetoshi Morita[11], Masahira Hattori[4] & Hiroshi Ohno[1,2,12]

The human gut is colonized with a wide variety of microorganisms, including species, such as those belonging to the bacterial genus *Bifidobacterium*, that have beneficial effects on human physiology and pathology[1–3]. Among the most distinctive benefits of bifidobacteria are modulation of host defence responses and protection against infectious diseases[4–6]. Nevertheless, the molecular mechanisms underlying these effects have barely been elucidated. To investigate these mechanisms, we used mice associated with certain bifidobacterial strains and a simplified model of lethal infection with enterohaemorrhagic *Escherichia coli* O157:H7, together with an integrated 'omics' approach. Here we show that genes encoding an ATP-binding-cassette-type carbohydrate transporter present in certain bifidobacteria contribute to protecting mice against death induced by *E. coli* O157:H7. We found that this effect can be attributed, at least in part, to increased production of acetate and that translocation of the *E. coli* O157:H7 Shiga toxin from the gut lumen to the blood was inhibited. We propose that acetate produced by protective bifidobacteria improves intestinal defence mediated by epithelial cells and thereby protects the host against lethal infection.

Enterohaemorrhagic *Escherichia coli* (EHEC) causes illnesses ranging from mild diarrhoea to severe diseases such as haemorrhagic colitis and haemolytic uraemic syndrome[7,8]. EHEC O157:H7, which produces Shiga toxin (Stx), is the major EHEC serotype responsible for public health problems worldwide[9]. Germ-free mice are a suitable model for analysing the mechanism of infection with this bacterium, which is denoted *E. coli* O157 throughout. Studies using this model have shown previously that Stx (both Stx1 and Stx2) produced by *E. coli* O157 is a crucial factor in lethal infection[10] and that pretreatment with certain probiotics, including bifidobacteria, protects mice against death[11–13]. However, the protective mechanism of bifidobacteria remains unknown.

When germ-free mice were fed *E. coli* O157, they died within 7 days. However, mice survived if they had been colonized, 7 days before inoculation with *E. coli* O157, with *Bifidobacterium longum* subsp. *longum* JCM 1217^T (denoted BL) (Fig. 1a and Supplementary Table 1). By contrast, another strain of bifidobacteria, *Bifidobacterium adolescentis* JCM 1275^T (BA), failed to prevent *E. coli* O157-induced death under the same conditions. In these two groups of mice—denoted BL+O157 mice and BA+O157 mice—there was no significant difference in several physiological and pathological markers in the gut: the number of *E. coli* O157 and the number of bifidobacteria, the concentration of Stx2 protein (the type of Stx produced by the *E. coli* strain studied), the expression level of *E. coli* O157 virulence genes, the amounts of mucin and immunoglobulin A (IgA), and the pH (Fig. 1b–d and Supplementary Fig. 1). Nevertheless, the serum concentration of Stx2 was markedly lower in BL+O157 mice than in BA+O157 mice (Fig. 1e), suggesting that BL, but not BA, promotes epithelial defence functions that prevent the translocation of Stx2 into the blood.

Consistent with this idea, histological analysis showed a slight inflammation, characterized by a reduction in the number of goblet cells and an infiltration with inflammatory cells, only in the distal colon of the dying mice that been administered *E. coli* O157 alone (O157 mice) and in the BA+O157 mice but not in the surviving BL+O157 mice (Supplementary Fig. 2a, b). Gene expression profiling of the distal colonic epithelium, followed by multivariate partial least squares-discriminant analysis (PLS-DA), also showed substantial upregulation of inflammation-related genes in O157 and BA+O157 mice, even as early as 1 day after administration of *E. coli* O157, when no obvious microscopic inflammation was evident (Supplementary Figs 2c and 3 and Supplementary Tables 2 and 3). This upregulation of inflammation-related genes coincided with increased epithelial cell apoptosis in O157 and BA+O157 mice (Supplementary Fig. 2d), suggesting that *E. coli* O157 provokes apoptosis of these cells before mucosal inflammation can occur and that such inflammation does not occur if BL has been administered.

It was unclear how BL, but not BA, prevents *E. coli* O157-induced epithelial cell apoptosis. We thought that differential metabolite production by BL and BA in the gut environment might be involved in this process. To address this possibility, we performed PLS-DA of the metabolic profiles of faeces from mice that had been monoassociated with each of four bifidobacterial strains: BL (which prevents infection with *E. coli* O157); *B. longum* subsp. *infantis* 157F (BF)[13] (preventive); BA (non-preventive); and *B. longum* subsp. *infantis* JCM 1222^T (BT)[13] (non-preventive). We found a striking difference in the faecal metabolite composition between mice that had been administered the preventive strains and those that had received the non-preventive strains (Fig. 2a). Loading-plot analysis and ^{1}H–^{13}C correlation NMR measurement identified carbohydrates as the main metabolites that differed between mice associated with the preventive bifidobacterial strains and the non-preventive ones (Supplementary Fig. 4 and Supplementary Table 4). The efficiency of carbohydrate consumption by bifidobacteria correlated with their ability to prevent *E. coli* O157-induced death.

Short-chain fatty acids are the major end products of carbohydrate metabolism in bifidobacteria. Indeed, the concentration of acetate, but not lactate or formate, was significantly higher in the faeces of mice associated with the preventive strains than in those associated with the non-preventive strains (Fig. 2b). Butyrate and propionate were not

[1]Laboratory for Epithelial Immunobiology, RIKEN Research Center for Allergy and Immunology, 1-7-22 Suehiro-cho, Tsurumi-ku, Yokohama, Kanagawa 230-0045, Japan. [2]Graduate School of Nanobioscience, Yokohama City University, 1-7-29 Suehiro-cho, Tsurumi-ku, Yokohama, Kanagawa 230-0045, Japan. [3]MetaSystems Research Team, RIKEN Advanced Science Institute, 1-7-22 Suehiro-cho, Tsurumi-ku, Yokohama, Kanagawa 230-0045, Japan. [4]Graduate School of Frontier Sciences, The University of Tokyo, 5-1-5 Kashiwanoha, Kashiwa, Chiba 277-8561, Japan. [5]Advanced NMR Metabomics Research Team, RIKEN Plant Science Center, 1-7-22 Suehiro-cho, Tsurumi-ku, Yokohama, Kanagawa 230-0045, Japan. [6]Graduate School of Agricultural and Life Sciences, The University of Tokyo, 1-1-1 Yayoi, Bunkyo-ku, Tokyo 113-8657, Japan. [7]Graduate School of Medicine, Osaka University, 2-2 Yamada-oka, Suita, Osaka 565-0871, Japan. [8]Preventative Health National Research Flagship, CSIRO Food and Nutritional Sciences, Adelaide, South Australia 5000, Australia. [9]The United Graduate School of Agricultural Science, Gifu University, 1-1 Yanagido, Gifu 501-1193, Japan. [10]Graduate School of Bioagricultural Sciences, Nagoya University, Furo-cho, Chikusa-ku, Nagoya, Aichi 464-8601, Japan. [11]School of Veterinary Medicine, Azabu University, 1-17-71 Fuchinobe, Sagamihara, Kanagawa 229-8501, Japan. [12]Graduate School of Medicine, Chiba University, 1-8-1 Inohana, Chuo-ku, Chiba 260-8670, Japan.

©2011 Macmillan Publishers Limited. All rights reserved

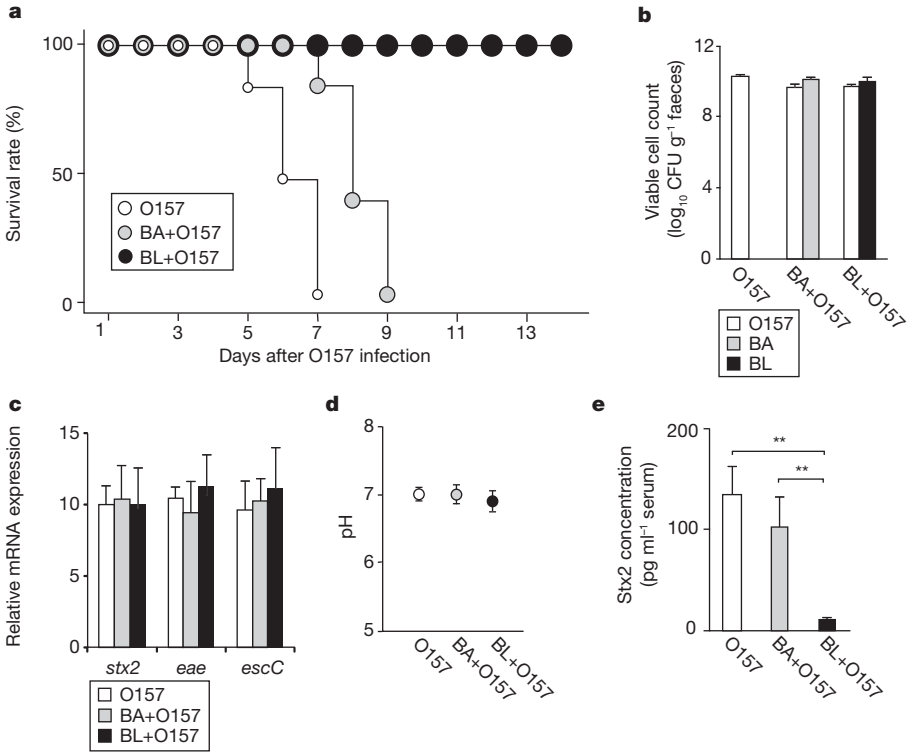

Figure 1 | Effect of preventive and non-preventive bifidobacteria against lethal infection with *E. coli* O157. **a**, Survival rate of mice after infection with *E. coli* O157: germ-free BALB/c mice (O157); mice associated with the preventive *B. longum* subsp. *longum* JCM 1217^{T} (BL+O157); and with the non-preventive *Bifidobacterium adolescentis* JCM 1275^{T} (BA+O157). $n = 10$. **b**, Number of *E. coli* O157 and bifidobacteria in faeces. CFU, colony-forming unit. **c**, Quantitative RT–PCR (PCR with reverse transcription) analysis of expression of the *E. coli* O157 virulence genes encoding Stx2 (*stx2*), intimin (*eae*) and a type III secretion system component (*escC*) in these mice. Messenger RNA expression values are expressed relative to the percentage of *E. coli* O157 16S ribosomal RNA. **d**, pH of the caecal contents. **e**, Stx2 concentration in the serum. *P* value was determined using the Kruskal–Wallis test followed by the Scheffé test. **, $P < 0.01$. **b**–**e**, Error bars, s.e.m. ($n = 3$).

detected in the faeces of any of these groups of mice (data not shown). These results suggest a positive correlation between the amount of faecal acetate and the resistance of mice to infection with *E. coli* O157. Covariation analysis of the transcriptome of the colonic epithelium (Supplementary Figs 5 and 6 and Supplementary Table 5) and the faecal metabolome of BL-monoassociated mice and BA-monoassociated mice (Supplementary Fig. 7) indicated that the expression level of mouse genes such as *Apoe*, *C3* and *Pla2g2a* strongly correlates with the amount of faecal acetate. The transcription of *Apoe*, *C3* and *Pla2g2a* is known to be upregulated by activation of retinoid X receptor, which has a central role in the transcriptional control of cellular energy metabolism[14–16] and in the anti-inflammatory response[17–20]. Experiments using human colonic epithelial (Caco-2) cells confirmed that acetate could induce the expression of these three genes (Fig. 2c). Additionally, acetate prevented the reduction in transepithelial electrical resistance resulting from *E. coli* O157-induced cell death and the translocation of Stx2 from the apical to the basolateral side of colonic epithelial cells, without affecting the growth rate of *E. coli* O157 or the expression level of several virulence genes of *E. coli* O157 (Fig. 2d–f and Supplementary Fig. 8). These data strongly suggest that acetate produced in large amounts by the preventive bifidobacteria exerts its action on the colonic epithelium by inducing anti-inflammatory and/or anti-apoptotic effects, blocking the translocation of the lethal dose of Stx2 to the blood.

To gain genetic insight into how the preventive strains efficiently consume carbohydrates and produce acetate, we determined the complete genome sequences of BL, BF and BT[21] and compared them with the sequences of BA and another preventive strain, *B. longum* subsp. *longum* NCC 2705 (BN)[22] (which were available from public databases) (Supplementary Tables 1 and 6). Reciprocal BLASTP comparison between the gene sets of these five genomes identified five syntenic loci that are present in the preventive bifidobacteria (BL, BF and BN) but absent from the non-preventive ones (BA and BT) (Supplementary Table 7). All five loci contained genes encoding ATP-binding cassette (ABC)-type carbohydrate transporters. Among them, the genes assigned to COG1879, COG1172 and COG1129 (the clusters of orthologous groups from the NCBI COGs database) at loci 1 and 5 were specific to the preventive bifidobacteria (Fig. 3a). At the other three loci, by contrast, paralogous genes were also present in the genomes of the non-preventive bifidobacteria (Supplementary Table 8).

Substrates for the preventive-bifidobacteria-specific transporters were predicted, by *in silico* analysis by another research group, to be ribose, fructose, mannose and many other sugars[23,24]. Substrates for the transporters commonly expressed in the preventive and non-preventive bifidobacteria were predicted to be fructo-oligosaccharide and lactose[23] (Supplementary Table 7). Correspondingly, *in vitro* metabolic profiling using ^{13}C-labelled glucose and fructose, followed by PLS-DA, revealed both a significantly higher rate of consumption of fructose and production of acetate in the preventive strains than in the non-preventive strains (Fig. 3b, c and Supplementary Table 9). Consistent with the predicted substrate specificity of the transporters, mannose, but not fructo-oligosaccharide or lactose, was also a specific substrate for the preventive bifidobacteria (Supplementary Table 10). Of the two preventive bifidobacteria-specific carbohydrate transporters (those encoded at loci 1 and 5) (Fig. 3a), the expression of the genes BL0033 and BL0034 by BN has been reported to be highly induced by fructose[24]. We confirmed that fructose upregulated expression of BL0033–BL0036, but not BL1691–BL1696, in BN (Supplementary Fig. 9a), and we found that BL0033 was expressed by the preventive bifidobacteria in the mouse distal colon (Supplementary Fig. 9b). These data suggest that the genes BL0033–BL0036 are involved in preventing *E. coli* O157-induced death of mice by, at least, BN.

©2011 Macmillan Publishers Limited. All rights reserved

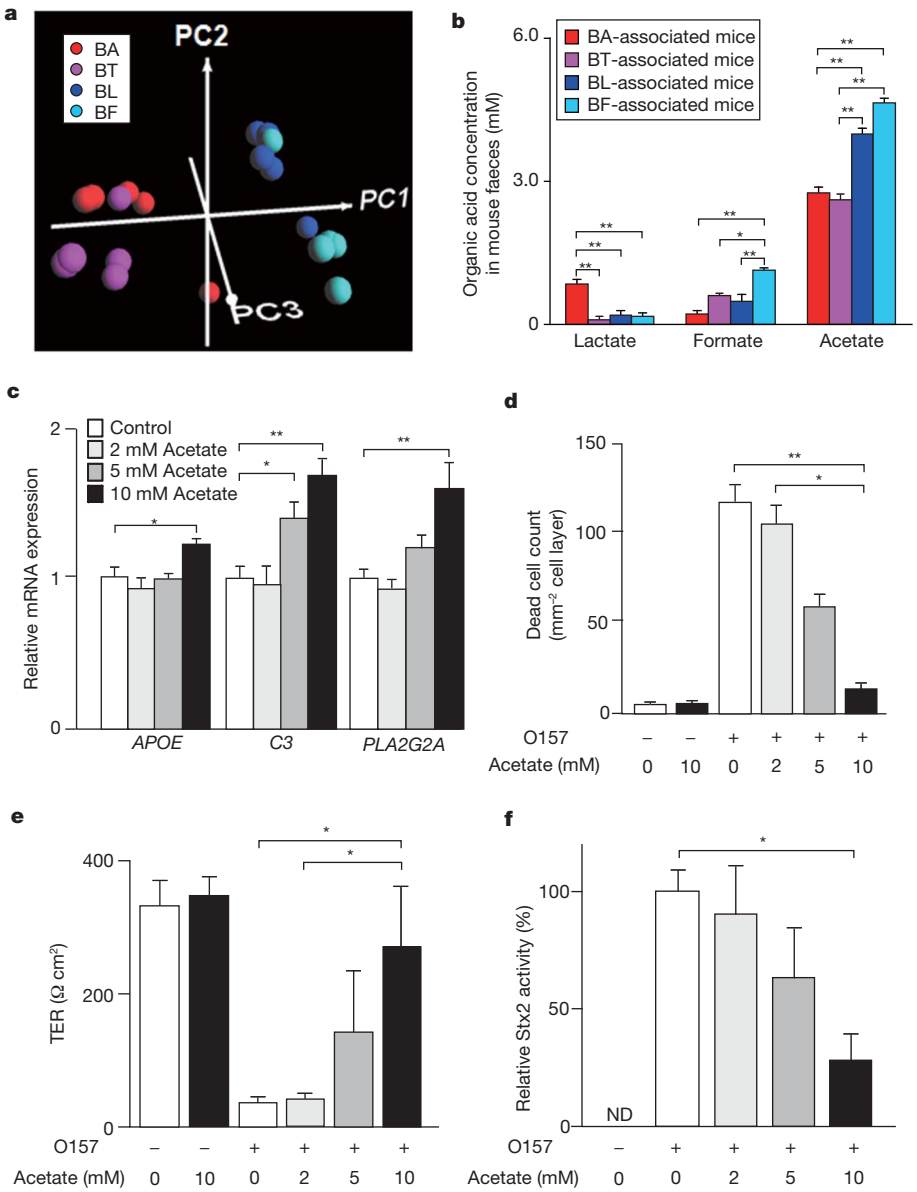

Figure 2 | Identification of acetate as causative substance for protection provided by preventive bifidobacteria. **a**, PLS-DA on metabolome data from mouse faeces 7 days after inoculation of each preventive and non-preventive bifidobacterial strain into germ-free mice ($n = 5$). Proportions of the first (PC1), second (PC2) and third (PC3) components are 66.5%, 11.2% and 9.1%, respectively. **b**, Organic acid concentrations in mouse faeces, as determined by high-performance liquid chromatography. **c**, Quantitative RT–PCR analysis of *APOE, C3* and *PLA2G2A* gene expression in Caco-2 cells in the absence or presence of the indicated concentration of acetate. The orthologues of these genes were upregulated in the colonic epithelium of mice associated with preventive bifidobacteria (Supplementary Table 5). Gene expression levels are expressed as values relative to the control (0 mM acetate). **d**, The number of dead cells in polarized Caco-2 cells 8 h after infection with *E. coli* O157 in the absence or presence of the indicated concentration of acetate. **e**, Transepithelial electrical resistance (TER) of polarized Caco-2 cells 16 h after infection with *E. coli* O157 in the absence or presence of the indicated concentration of acetate. **f**, Relative Stx2 activity in the basolateral side of polarized Caco-2 cell culture media 16 h after infection with *E. coli* O157 in the absence or presence of the indicated concentration of acetate. Activity is expressed as a percentage of activity in control cells (infected with *E. coli* O157 and treated with 0 mM acetate). **b**–**f**, Error bars, s.e.m. ($n = 3$). *P* values were determined using the one-way analysis of variance (ANOVA) test followed by Tukey's test (**b**, **c**) or the Kruskal–Wallis test followed by the Scheffé test (**d**–**f**). *, $P < 0.05$; **, $P < 0.01$. ND, not detected.

To test this, we generated a strain of BN in which BL0033 had been knocked out (denoted BNKO) using homologous recombination (Supplementary Figs 9a and 10). *In vitro* culture of BNKO showed a significant reduction in capacity to catabolize fructose and in acetate production compared with BN (Fig. 4a). Accordingly, BNKO did not prevent Caco-2 cell death induced by *E. coli* O157 (Supplementary Fig. 11). More importantly, the survival rate of BNKO-associated mice after infection with *E. coli* O157 was also significantly less than that of BN-associated mice, consistent with the lower acetate concentration in the faeces of BNKO-associated mice (Fig. 4b, c).

We also generated a strain of BA strain that exogenously expressed BL0033–BL0036 (denoted BAtg). After infection with *E. coli* O157, BAtg-associated mice survived slightly (but significantly) longer than BA-associated mice (Fig. 4d). The moderate effect of BAtg is probably caused by a modest increase in acetate produced from fructose because of the lower expression of BL0033–BL0036 in BAtg than in BN, in the presence of fructose (Fig. 4e and Supplementary Fig. 9a). Finally, we asked whether an increased amount of acetate in the distal colon could protect mice against *E. coli* O157-induced death. We fed BA+O157 mice a diet supplemented with acetylated starch, which is gradually hydrolysed, releasing acetate in the intestinal tract[25]. Administration of the acetylated starch significantly increased the amount of acetate in the faeces and improved the survival rate of BA-associated mice in response to *E. coli* O157, suggesting that the amount of acetate is crucial for this protection (Fig. 4f, g).

Short-chain fatty acids generated by commensal bacteria have long been implicated in having a variety of beneficial effects on the host, including trophic and anti-inflammatory effects on the gut *in vitro*[1,5,12,26,27] and *in vivo*[28]. Our findings suggest that bacterial acetate acts *in vivo* to promote the defence functions of host epithelial cells. Of more importance is the identification of carbohydrate transporters that confer a probiotic effect on bifidobacterial strains. These 'probiotic transporters' are likely to be present in only a subset of *B. longum*, and genes encoding proteins that are highly similar to these probiotic transporters were also identified in several human gut microbiomes[29] (Supplementary Table 11). Both the preventive and non-preventive bifidobacteria can produce enough acetate in the presence of glucose, and this is probably what takes place in the proximal part of the colon. In the distal colon, however, the glucose supply has been exhausted, and only the bifidobacteria equipped with probiotic transporters can produce enough acetate, through catabolizing the fructose that is present (Supplementary Fig. 12). As demonstrated in this study, a simplified

©2011 Macmillan Publishers Limited. All rights reserved

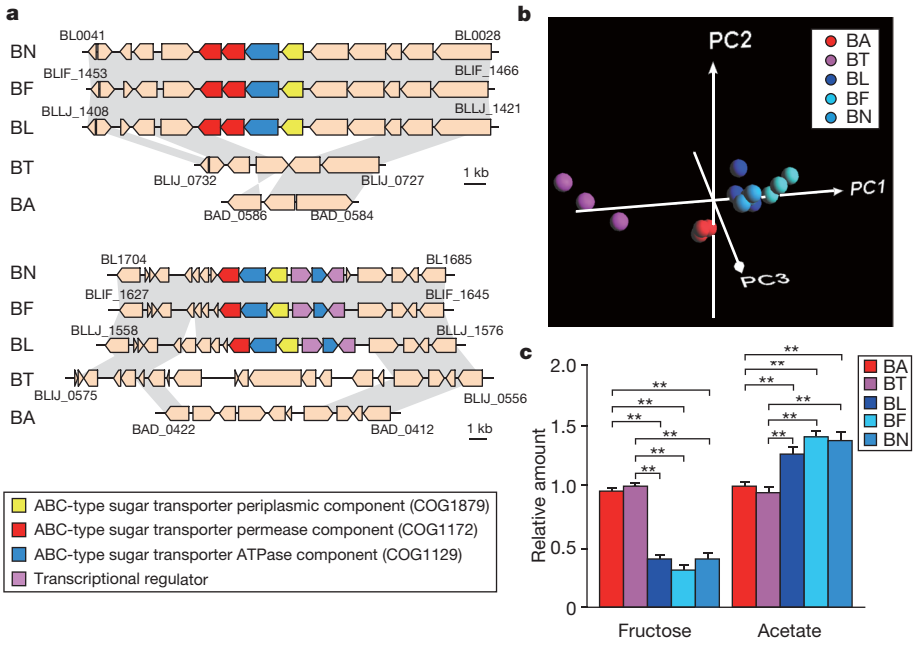

Figure 3 | Genomic and metabolic profiling of the bifidobacterial strains. **a**, Comparison of the regions containing the genes that encode specific ABC-type carbohydrate transporters in the sequenced bifidobacterial strains. Genes and their orientations are depicted with arrows. Grey bars indicate orthologous regions. **b**, PLS-DA on metabolome data from bifidobacterial strains cultured for 12 h in ^{13}C-labelled medium *in vitro*. Proportions of the first (PC1), second (PC2) and third (PC3) components are 73.1%, 16.8% and 4.0%, respectively. The top five loading coefficients of ^{1}H–^{13}C correlation NMR cross peaks are shown in Supplementary Table 9. **c**, Relative amount of fructose or acetate present in the medium for the five bifidobacterial strains after 12 h incubation *in vitro* ($n = 3$). The amounts of fructose and acetate are shown as values relative to those for BA. Error bars, s.e.m. *P* values were determined using the one-way ANOVA test followed by Tukey's test. **, $P < 0.01$.

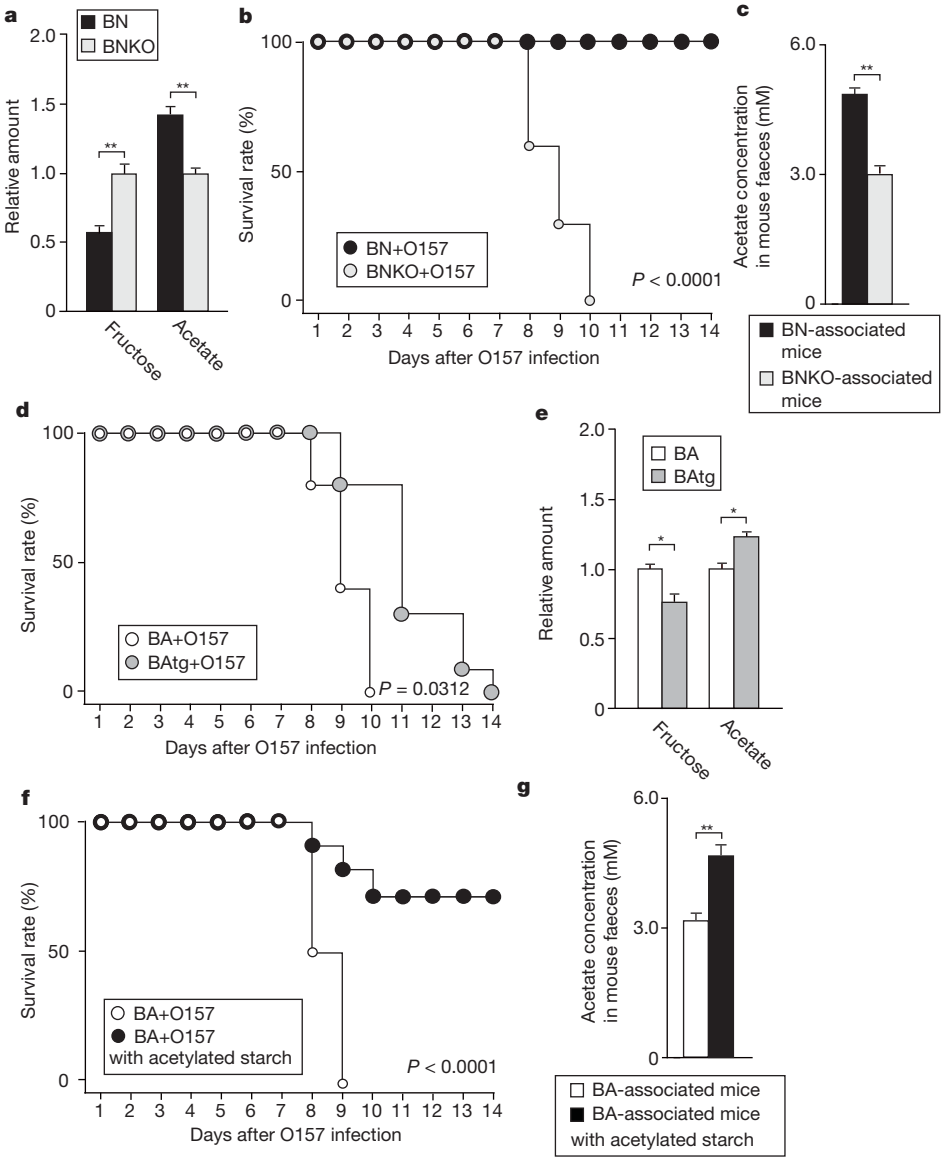

Figure 4 | Functional analysis of the ABC-type carbohydrate transporter. **a**, Amount of fructose and acetate present in the medium for BN and BNKO after 12 h incubation *in vitro* ($n = 5$). Data are expressed relative to the amount for BNKO. **b**, Survival rate of BN- and BNKO-associated mice after infection with *E. coli* O157 ($n = 10$). **c**, Acetate concentration in the faeces of BN- and BNKO-associated mice ($n = 5$). **d**, Survival rate of BA- and BAtg-associated mice after infection with *E. coli* O157 ($n = 10$). **e**, Amount of fructose and acetate present in the medium for BA and BAtg after 12 h incubation *in vitro* ($n = 5$). Data are expressed relative to the amount for BA. **f**, Survival rate of BA+O157 mice fed with a control synthetic diet or a modified synthetic diet—in which 15% starch was replaced with acetylated starch—for 1 week before infection with *E. coli* O157 ($n = 10$). **g**, Acetate concentration in the faeces of BA-associated mice fed on a control diet or starch-modified diet ($n = 5$). **a**, **c**, **e**, **g**, Error bars, s.e.m. *P* values were determined using Student's *t*-test. *, $P < 0.05$; **, $P < 0.01$. **b**, **d**, **f**, *P* values were determined using the Kaplan–Meier method followed by the log-rank test.

©2011 Macmillan Publishers Limited. All rights reserved

animal model system coupled with multiple 'omics' technologies can provide a powerful strategy for dissecting host–microbe cross-talk in the complex gut ecosystem.

METHODS SUMMARY

Animals. Germ-free BALB/c mice were housed in gnotobiotic isolators and fed an autoclaved standard rodent chow diet (CMF, Oriental Yeast). All experiments were performed using protocols approved by the University of Tokyo Animal Studies Committee. Male or female germ-free mice of 8–16 weeks of age were colonized with a single gavage of 10^8 colony-forming units (CFU) of bifidobacteria. For infection with *E. coli* O157, mice that were germ free or had been monoassociated with bifidobacteria (for 7 days) were orally inoculated with a single gavage of 10^4 CFU of *E. coli* O157:H7 strain 44^{Rf}.

Metabolic profiling. Faecal metabolites were extracted by gentle shaking of faeces with 100 mM potassium phosphate buffer containing 90% deuterium oxide and 1 mM sodium 2,2-dimethyl-2-silapentane-5-sulphonate as the chemical-shift reference compound ($\delta = 0.0$ p.p.m.). They were then analysed by ^{1}H-NMR and ^{1}H–^{13}C correlation NMR spectroscopy. PLS-DA, a regression extension of the classical principal component analysis that is appropriate to the metabolome data set, was run with R software using the PLS package (v2.0) and the 'SIMPLS' method. Briefly, the normalized metabolome data set was imported into the R software. Variance and regression were computed in a class-supervised manner, and principal component (PC) scores were determined. Data were visualized as PC score plots, with the PC1 axis showing most of the differences among the samples, whereas PC2 and PC3 corresponded to factors with decreasing contribution to the differences.

Full Methods and any associated references are available in the online version of the paper at www.nature.com/nature.

Received 11 September 2009; accepted 4 November 2010.

1. Picard, C. *et al.* Bifidobacteria as probiotic agents—physiological effects and clinical benefits. *Aliment. Pharmacol. Ther.* **22,** 495–512 (2005).
2. Ventura, M. *et al.* Genome-scale analyses of health-promoting bacteria: probiogenomics. *Nature Rev. Microbiol.* **7,** 61–71 (2009).
3. Jia, W., Li, H., Zhao, L. & Nicholson, J. K. Gut microbiota: a potential new territory for drug targeting. *Nature Rev. Drug Discov.* **7,** 123–129 (2008).
4. Mazmanian, S. K. & Kasper, D. L. The love–hate relationship between bacterial polysaccharides and the host immune system. *Nature Rev. Immunol.* **6,** 849–858 (2006).
5. Saulnier, D. M., Spinler, J. K., Gibson, G. R. & Versalovic, J. Mechanisms of probiosis and prebiosis: considerations for enhanced functional foods. *Curr. Opin. Biotechnol.* **20,** 135–141 (2009).
6. Sonnenburg, J. L., Chen, C. T. & Gordon, J. I. Genomic and metabolic studies of the impact of probiotics on a model gut symbiont and host. *PLoS Biol.* **4,** e413 (2006).
7. Garmendia, J., Frankel, G. & Crepin, V. F. Enteropathogenic and enterohemorrhagic *Escherichia coli* infections: translocation, translocation, translocation. *Infect. Immun.* **73,** 2573–2585 (2005).
8. Tarr, P. I., Gordon, C. A. & Chandler, W. L. Shiga-toxin-producing *Escherichia coli* and haemolytic uraemic syndrome. *Lancet* **365,** 1073–1086 (2005).
9. Kitajima, H., Ida, S. & Fujimura, M. Daily bowel movements and *Escherichia coli* O157 infection. *Arch. Dis. Child.* **87,** 335–336 (2002).
10. Eaton, K. A. *et al.* Pathogenesis of renal disease due to enterohemorrhagic *Escherichia coli* in germ-free mice. *Infect. Immun.* **76,** 3054–3063 (2008).
11. Asahara, T. *et al.* Probiotic bifidobacteria protect mice from lethal infection with Shiga toxin-producing *Escherichia coli* O157:H7. *Infect. Immun.* **72,** 2240–2247 (2004).
12. Gagnon, M., Kheadr, E. E., Dabour, N., Richard, D. & Fliss, I. Effect of *Bifidobacterium thermacidophilum* probiotic feeding on enterohemorrhagic *Escherichia coli* O157:H7 infection in BALB/c mice. *Int. J. Food Microbiol.* **111,** 26–33 (2006).
13. Yoshimura, K., Matsui, T. & Itoh, K. Prevention of *Escherichia coli* O157:H7 infection in gnotobiotic mice associated with *Bifidobacterium* strains. *Antonie Van Leeuwenhoek* **97,** 107–117 (2010).
14. Li, J., Pircher, P. C., Schulman, I. G. & Westin, S. K. Regulation of complement C3 expression by the bile acid receptor FXR. *J. Biol. Chem.* **280,** 7427–7434 (2005).
15. Laffitte, B. A. *et al.* LXRs control lipid-inducible expression of the apolipoprotein E gene in macrophages and adipocytes. *Proc. Natl Acad. Sci. USA* **98,** 507–512 (2001).
16. Antonio, V., Janvier, B., Brouillet, A., Andreani, M. & Raymondjean, M. Oxysterol and 9-*cis*-retinoic acid stimulate the group IIA secretory phospholipase A_2 gene in rat smooth-muscle cells. *Biochem. J.* **376,** 351–360 (2003).
17. Zelcer, N. & Tontonoz, P. Liver X receptors as integrators of metabolic and inflammatory signaling. *J. Clin. Invest.* **116,** 607–614 (2006).
18. Sethi, S. *et al.* Oxidized omega-3 fatty acids in fish oil inhibit leukocyte–endothelial interactions through activation of PPARα. *Blood* **100,** 1340–1346 (2002).
19. Staels, B. *et al.* Activation of human aortic smooth-muscle cells is inhibited by PPARα but not by PPARγ activators. *Nature* **393,** 790–793 (1998).
20. Delerive, P., Gervois, P., Fruchart, J. C. & Staels, B. Induction of IκBα expression as a mechanism contributing to the anti-inflammatory activities of peroxisome proliferator-activated receptor-α activators. *J. Biol. Chem.* **275,** 36703–36707 (2000).
21. Sela, D. A. *et al.* The genome sequence of *Bifidobacterium longum* subsp. *infantis* reveals adaptations for milk utilization within the infant microbiome. *Proc. Natl Acad. Sci. USA* **105,** 18964–18969 (2008).
22. Schell, M. A. *et al.* The genome sequence of *Bifidobacterium longum* reflects its adaptation to the human gastrointestinal tract. *Proc. Natl Acad. Sci. USA* **99,** 14422–14427 (2002).
23. Parche, S. *et al.* Sugar transport systems of *Bifidobacterium longum* NCC 2705. *J. Mol. Microbiol. Biotechnol.* **12,** 9–19 (2007).
24. Yuan, J. *et al.* A proteome reference map and proteomic analysis of *Bifidobacterium longum* NCC 2705. *Mol. Cell. Proteomics* **5,** 1105–1118 (2006).
25. Annison, G., Illman, R. J. & Topping, D. L. Acetylated, propionylated or butyrylated starches raise large bowel short-chain fatty acids preferentially when fed to rats. *J. Nutr.* **133,** 3523–3528 (2003).
26. Tedelind, S., Westberg, F., Kjerrulf, M. & Vidal, A. Anti-inflammatory properties of the short-chain fatty acids acetate and propionate: a study with relevance to inflammatory bowel disease. *World J. Gastroenterol.* **13,** 2826–2832 (2007).
27. Kles, K. A. & Chang, E. B. Short-chain fatty acids impact on intestinal adaptation, inflammation, carcinoma, and failure. *Gastroenterology* **130,** S100–S105 (2006).
28. Maslowski, K. M. *et al.* Regulation of inflammatory responses by gut microbiota and chemoattractant receptor GPR43. *Nature* **461,** 1282–1286 (2009).
29. Kurokawa, K. *et al.* Comparative metagenomics revealed commonly enriched gene sets in human gut microbiomes. *DNA Res.* **14,** 169–181 (2007).

Supplementary Information is linked to the online version of the paper at www.nature.com/nature.

Acknowledgements We thank H. Kitamura and M. E. Mariotti-Ferrandiz for discussions and for reading the manuscript; T. Morita for suggestions; and C. Nishigaki, M. Ohmae, Y. Chiba, T. Kato, H. Shima, A. Nakano, K. Sakaguchi, K. Furuya, C. Yoshino, H. Inaba, E. Iioka, K. Motomura and Y. Hattori for technical support. This research was supported in part by grants from the Ministry of Education, Culture, Sports, Science and Technology of Japan: a Grant-in-Aid for Scientific Research on Priority Areas 'Comprehensive Genomics' (M.H.), 'Membrane Traffic' (H.O.) and 'Matrix of Infectious Phenomena' (K.H.); Young Scientists (S.F., K.H. and J.K.); Challenging Exploratory Research (J.K.); Scientific Research (H.O.); and Scientific Research on Innovative Areas 'Intracellular Logistics' (H.O.). This work was also supported in part by a RIKEN President's Special Research Grant (J.K.); a RIKEN DRI Research Grant (S.F.); a CREST grant from the Japan Science and Technology Agency (J.K.); the Danone Institute of Japan (H.O.); the Institute for Fermentation, Osaka (S.F.); the Kieikai Research Foundation (S.F.); the Naito Foundation (S.F.); the Nestlé Nutrition Council, Japan (S.F.); the Sasakawa Scientific Research Grant from the Japan Science Society (S.F. and Y.N.); the Yakult Bio-Science Foundation (S.F.); the Academic Frontier Project for Private Universities (Matching Fund Subsidy (H.M.)); and the Private University Scientific Foundation (H.M.).

Author Contributions S.F., K.I., M.H. and H.O. conceived and designed the experiments. S.F., Y.N., K.H., K.Y., K.O., H.M. and K.I. performed the experiments. S.F., H.T. and Y.N. analysed the data. T.T., J.M.C., D.L.T., T.S., T.D.T., J.K. and M.H. contributed reagents, materials and analysis tools. S.F., H.T., K.H., T.D.T., M.H. and H.O. wrote the paper.

Author Information Microarray data have been deposited in the NCBI Gene Expression Omnibus under accession number GSE13061. Sequences for the *B. longum* genomes have been deposited in the DNA Data Bank of Japan, GenBank and the EMBL Nucleotide Sequence Database under accession numbers AP010888 (BL), AP010889 (BT) and AP010890–AP010892 (BF). Reprints and permissions information is available at www.nature.com/reprints. The authors declare no competing financial interests. Readers are welcome to comment on the online version of this article at www.nature.com/nature. Correspondence and requests for materials should be addressed to H.O. (ohno@rcai.riken.jp) or M.H. (hattori@k.u-tokyo.ac.jp).

©2011 Macmillan Publishers Limited. All rights reserved

METHODS

Bacterial strains, cell lines and culture conditions. *B. longum* subsp. *longum* JCM 1217^T (BL), *B. longum* subsp. *infantis* JCM 1222^T (BT) and *B. adolescentis* JCM 1275^T (BA) were purchased from the Japan Collection of Microorganisms. *B. longum* subsp. *longum* NCC 2705 (BN) was provided by the Nestlé Research Center. *B. longum* subsp. *infantis* 157F (BF) was isolated from the faeces of a human infant[13]. *E. coli* O157:H7 strain 44^{Rf} (*E. coli* O157), a rifampicin-resistant mutant, was originally derived from bovine faeces[13]. This strain does not produce Stx1. Bifidobacteria and *E. coli* O157 were cultured anaerobically in blood liver (BL) agar (Nissui) and tryptic soy (TS) agar (BBL, Becton Dickinson), respectively[13].

Vero cells and Caco-2 cells were purchased from the American Type Culture Collection. They were grown as a monolayer in the medium DMEM (GIBCO) supplemented with 10% FBS and 1% penicillin-streptomycin-glutamine (GIBCO). Cultures were maintained in plastic dishes at 37 °C in a 5% CO_2 atmosphere.

Counting the number of bacteria in faeces. Unless stated otherwise, the faecal samples were directly collected from mice just after a bowel movement. These samples were then immediately used for several analyses. Faecal suspensions were homogenized with anaerobic solution A (4.5 g l^{-1} KH_2PO_4, 6.0 g l^{-1} Na_2HPO_4, 12.5 g l^{-1} L-cysteine-HCl, 0.5 g l^{-1} Tween 80 and 0.75 g l^{-1} Bacto Agar (BBL)) (1:50 dilution). Serial tenfold dilutions were prepared, and a 50 µl aliquot of each dilution was spread on TS agar plates (for *E. coli* O157) or BL agar plates (for bifidobacteria). The plates were incubated at 37 °C anaerobically, and the CFU were enumerated[13].

Vero cell bioassay for Stx2 cytotoxicity. Stx2 cytotoxicity was determined in 96-well microtitre plates, as previously described[30]. Cell morphology was observed under a phase contrast microscope. Shiga toxin (100 ng ml^{-1}; VTEC-RPLA test, Denka Seiken) was used as a standard.

Measurement of mucin, total IgA, pH and organic acids. Crude mucin was isolated from mouse caecal contents and analysed by SDS–PAGE[31]. Caecal IgA was determined using the mouse IgA ELISA quantitation set (Bethyl Laboratories). Caecal pH was measured with a compact pH meter (Model C-1, Horiba). Organic acid concentrations of faecal contents were determined by NMR spectroscopy (DRX-700 spectrometer, Bruker BioSpin) and high-performance liquid chromatography (L-7000, Hitachi)[31].

Immunohistochemistry. Paraformaldehyde-fixed, frozen sections of mouse large intestine were stained with anti-mouse CD4, CD11b and CD11c monoclonal antibodies (BD Biosciences) and anti-Ki67 antiserum (Novocastra), as described previously[32]. For the TdT-mediated dUTP nick end labelling (TUNEL) staining, sections of mouse large intestine were fixed in 4% paraformaldehyde, frozen and then stained with the *in situ* cell death detection kit, fluorescein (Roche). For haematoxylin and eosin staining, sections of mouse large intestine were fixed in 10% formalin (Richard-Allan Scientific) and stained according to standard protocols.

Gene expression profiling of colonic epithelium. The colonic epithelium was isolated from the distal colon, as previously described[33]. Epithelial samples obtained from the colon of two mice from each group were combined, and total RNA was extracted according to standard protocols (Affymetrix). Targets were then prepared and hybridized to the GeneChip Mouse Genome 430 2.0 Array (Affymetrix) according to standard protocols. GeneChip data sets were analysed using GeneSpring GX 7.3.1 (Agilent). Array data were normalized using robust multi-array analysis considering guanine and cytosine content (GC-RMA) algorithms[34]. Probe sets categorized to A or B, which both target specific transcripts in the databases NCBI Reference Sequence (RefSeq) and NCBI GenBank, were used[35].

Self-organized mapping and hierarchical clustering analysis. Genes that were upregulated or downregulated twofold or more in O157, BA+O157 or BL+O157 mice compared with germ-free mice were selected (approximately 4,000 genes). Self-organized mapping and hierarchical clustering analysis were performed using GeneSpring GX 7.3.1. Briefly, in each experimental group, genes with similar relative expression values were clustered together, forming a cell. The resultant map allows easy visualization of the clusters. Hierarchical clustering analysis was then computed for the resultant maps to determine the similarity distances among the experimental groups.

PLS-DA on transcriptome data. The transcriptomic profiling data set that had been subjected to self-organized mapping analysis was imported into R software (R Foundation for Statistical Computing). Variance and regression were computed in a class-supervised manner, and principal component (PC) scores were determined[36]. Data were visualized as PC score plots, with the PC1 axis showing most of the differences among the samples, whereas PC2 and PC3 corresponded to factors with decreasing contribution to the differences.

Real-time quantitative RT–PCR. Total RNA was extracted and reverse-transcribed by using an RNeasy kit (QIAGEN) and RevaTra Ace (TOYOBO), respectively. Real-time PCR was performed using SYBR Premix Ex Taq (Takara) and primers specific for each gene (Supplementary Table 12). Assays were performed in triplicate using a Thermal Cycler Dice Real Time System (Takara).

^{1}H-NMR and ^{1}H–^{13}C correlation NMR measurements. For all '*in vivo*' experiments, faecal metabolites were extracted by gentle shaking of faeces in 100 mM potassium phosphate buffer containing 90% deuterium oxide and 1 mM sodium 2,2-dimethyl-2-silapentane-5-sulphonate as the chemical-shift reference compound ($\delta = 0.0$ p.p.m.). They were then analysed by ^{1}H-NMR and ^{1}H–^{13}C correlation NMR spectroscopy[37]. By contrast, all '*in vitro*' experiments were carried out using direct measurements of bacterial culture by ^{1}H-NMR and ^{1}H–^{13}C correlation NMR spectroscopy. Bacterial cells were cultivated in uniformly ^{13}C-labelled rich media (Spectra) supplemented with 0.5% (w/v) $^{13}C_6$-D-glucose (Spectra), 0.5% (w/v) $^{13}C_6$-D-fructose (Spectra) and 0.5% (w/v) ^{13}C,^{15}N Algal Amino Acid Mixture (Chlorella Industry). All *in vivo* and *in vitro* NMR experiments were conducted using a DRX-700 spectrometer equipped with a cryogenically cooled probe. The NMR spectra were processed with a procedure similar to that described previously[36–39]. Briefly, ^{1}H-NMR data were reduced by subdividing the spectra into sequential 0.04 p.p.m. designated regions between ^{1}H chemical shifts of 0.5–9.0 p.p.m. ^{1}H–^{13}C correlation NMR data were reduced by subdividing spectra into sequential bins of 0.3 p.p.m. in the f1 direction and 0.03 p.p.m. in f2 designated regions between ^{1}H chemical shifts of 0.5–9.0 p.p.m. and ^{13}C chemical shifts of 40–90 p.p.m., respectively. After exclusion of water resonance, each region was integrated and normalized to the total of all resonance integral regions (Supplementary Tables 13 and 14). Metabolite annotations were performed using our standard database[40,41].

***E. coli* O157 infection experiment in Caco-2 cells.** Caco-2 cells were grown on collagen-coated Transwell filter inserts (6.5 mm diameter, 0.4 µm pore size; Costar). During culture, transepithelial electrical resistance (TER) was monitored with an EVOM resistance reader (WPI)[42]. The cells were cultured for 7–12 days until stable TER values of 400 Ω cm^2 were obtained, indicating establishment of epithelial barrier function. The polarized Caco-2 cells were then pre-incubated with acetate for 72 h before infection with *E. coli* O157. Bacteria were added to the upper Transwell compartment at a multiplicity of infection (MOI) of 10 in complete medium without antibiotics. After the indicated incubation periods at 37 °C in 5% CO_2, the TER and Stx activity of the lower Transwell compartment were determined.

To count the dead cells, Caco-2 cells were grown on 6-well plastic plates for 7–12 days and treated with acetate at concentrations of 0–10 mM for 72 h before infection with *E. coli* O157 at an MOI of 10. After the indicated incubation periods, dead cells were stained with 0.5% (w/v) trypan blue and enumerated under a phase contrast microscope. In the co-culture experiments with bifidobacteria, polarized Caco-2 cells were pre-incubated with BN or BNKO for 12 h before infection with *E. coli* O157 at an MOI of 10. In these experiments, fructose was added at a final concentration of 3 mg ml^{-1} to glucose-free DMEM (D5030, Sigma-Aldrich) before culturing.

Genome sequencing. The genome sequences of BF, BT and BL were determined by a whole-genome shotgun strategy. We constructed small-insert (2 kb) and large-insert (10 kb) genomic libraries for the three genomes. We generated 26,880 (BF), 30,720 (BT) and 28,416 (BL) reads, each using 3730*xl* DNA Analyzers (Applied Biosystems), giving 7.8-, 6.3- and 7.6-fold coverage from both ends of the genomic clones, respectively. Sequence reads were assembled with the Phred-Phrap-Consed program[43], and gaps were closed by direct sequencing of clones that spanned the gaps or of PCR products amplified with oligonucleotide primers designed to anneal to each end of neighbouring contigs. The overall accuracy of the finished sequences was estimated to have an error rate of less than 1 in 10,000 bases (Phrap score, ≥ 40).

Genome informatics. An initial set of predicted protein-coding genes was identified using the program Glimmer 3.0 (ref. 44). Genes that were overlapping or <120 base pairs were eliminated. All predicted proteins were searched against a non-redundant protein database (nr, NCBI) using BLASTP (NCBI) with a bit-score cutoff of 60. The start codon of each protein-coding gene was manually refined from BLASTP alignments. Transfer RNA genes were predicted by the program tRNAscan-SE[45], and ribosomal RNA genes were detected by BLASTN analysis using known bifidobacterial rRNA sequences as queries. Orthology across whole genomes was determined using BLASTP reciprocal best hits with a bit-score cutoff of 60 in all-against-all comparisons of amino acid sequences.

Generation of BNKO, a BN strain deficient in the ABC-type carbohydrate transporter gene BL0033. A target vector containing two 1-kb genomic fragments flanking the spectinomycin-resistant gene was constructed with the plasmid pBluescript II SK (+). The targeting vector was introduced into BN by electroporation, and spectinomycin-resistant colonies were selected, as described previously[46]. The homologous recombination event in BNKO was confirmed by genomic PCR. Southern blotting further confirmed the absence of random integration of the targeting vector. The probes indicated in Supplementary Fig. 10a were

©2011 Macmillan Publishers Limited. All rights reserved

amplified by PCR using BN genomic DNA and the plasmid pKKT427 as templates, and the following primers: 5′-AACCAGCAGAAGGTGCTCATTG-3′ (forward) and 5′-AATGCGACGATCGACCAGGTC-3′ (reverse) for probe A; and 5′-TTGGTATGATTTTACCCGTGTCC-3′ (forward) and 5′-TTGGATCA GGAGTTGAGAGTGG-3′ (reverse) for probe B.

Generation of BAtg, a BA strain exogenously expressing the ABC-type carbohydrate transporter BL0033–BL0036. A 3.9-kb *Bifidobacterium–E. coli* shuttle vector, pKKT427 (ref. 47), carrying a spectinomycin-resistance gene, a multicloning site and two replication origins (including *repB* from *B. longum* and ColEI ori), was used to generate BAtg. DNA containing the ABC-type carbohydrate transporter (BL0033–BL0036) and the histone-like protein (HU) promoter, which was reported to be a high-level expression promoter in bifidobacteria[46], was cloned from BN. The regions encoding the ABC-type carbohydrate transporter and the HU promoter were amplified by PCR using the following primers: ABC-type carbohydrate transporter sense primer 5′-ATGAAGAATTGGAAGAAG GCC-3′ and antisense primer 5′-caacttttgtatacaaagttgCTATTTTTTATCTCCG CCGACC-3′; and HU promoter sense primer 5′-caagtttgtacaaaaaagcagTGGGC GCGGCGGCCATGAAG-3′ and antisense primer 5′-cttccaattcttcatAAAGCA TCCTTCTTGGGTCAGG-3′. Lower-case letters indicate pDONR vector sequences. The PCR products and linearized pDONR was ligated using the In-Fusion Advantage PCR Cloning Kit (Clontech). The pKKT427 plasmid containing the HU promoter and the ABC transporter gene (pKKT427-HU+BN) was constructed by using the Gateway system (Invitrogen) with the above pDONR vector. The pKKT427-HU+BN plasmid was transferred directly into BA by electroporation with a Gene Pulser apparatus (Bio-Rad)[46]. Transfected BA was grown under anaerobic conditions at 37 °C in BL agar containing 100 μg ml^{-1} spectinomycin.

Animal experiments with BAtg. Spectinomycin-resistant BA and *E. coli* O157 were generated by electroporation of a pKKT427 plasmid. To maintain a high copy number of pKKT427-HU+BN in BAtg, drinking water containing 1 mg ml^{-1} spectinomycin had been given to spectinomycin-resistant BA+O157 mice and spectinomycin-resistant BAtg+O157 mice 1 week before infection with spectinomycin-resistant *E. coli* O157.

Animal experiments with BA-associated mice fed on a starch-modified diet. BA+O157 mice were fed a control diet (AIN-93G synthetic diet) or a modified AIN-93G synthetic diet in which 15% (w/w) starch was replaced with acetylated starch (Starplus A, CSIRO) 1 week before infection with *E. coli* O157.

Statistical analyses. Differences between two or more groups were analysed by Student's *t*-test or the one-way analysis of variance (ANOVA) test followed by Tukey's test. When variances were not homogeneous, the data were analysed by the non-parametric Mann–Whitney *U* test or the Kruskal–Wallis test followed by the Scheffé test. The survival rate of mice associated with different bacteria was analysed using the Kaplan–Meier method. All statements indicating significant differences show at least a 5% level of probability.

30. Kongmuang, U., Honda, T. & Miwatani, T. Enzyme-linked immunosorbent assay to detect Shiga toxin of *Shigella dysenteriae* and related toxins. *J. Clin. Microbiol.* **25,** 115–118 (1987).
31. Morita, T., Tanabe, H., Takahashi, K. & Sugiyama, K. Ingestion of resistant starch protects endotoxin influx from the intestinal tract and reduces D-galactosamine-induced liver injury in rats. *J. Gastroenterol. Hepatol.* **19,** 303–313 (2004).
32. Hase, K. *et al.* Activation-induced cytidine deaminase deficiency causes organ-specific autoimmune disease. *PLoS ONE* **3,** e3033 (2008).
33. Hase, K. *et al.* Distinct gene expression profiles characterize cellular phenotypes of follicle-associated epithelium and M cells. *DNA Res.* **12,** 127–137 (2005).
34. Irizarry, R. A. *et al.* Summaries of Affymetrix GeneChip probe level data. *Nucleic Acids Res.* **31,** e15 (2003).
35. Hijikata, A. *et al.* Construction of an open-access database that integrates cross-reference information from the transcriptome and proteome of immune cells. *Bioinformatics* **23,** 2934–2941 (2007).
36. Tian, C. *et al.* Top-down phenomics of *Arabidopsis thaliana*: metabolic profiling by one- and two-dimensional nuclear magnetic resonance spectroscopy and transcriptome analysis of albino mutants. *J. Biol. Chem.* **282,** 18532–18541 (2007).
37. Fukuda, S. *et al.* Evaluation and characterization of bacterial metabolic dynamics with a novel profiling technique, real-time metabolotyping. *PLoS ONE* **4,** e4893 (2009).
38. Kikuchi, J., Shinozaki, K. & Hirayama, T. Stable isotope labeling of *Arabidopsis thaliana* for an NMR-based metabolomics approach. *Plant Cell Physiol.* **45,** 1099–1104 (2004).
39. Sekiyama, Y., Chikayama, E. & Kikuchi, J. Profiling polar and semi-polar plant metabolites throughout extraction processes using a combined solution-state and HR-MAS NMR approach. *Anal. Chem.* **82,** 1643–1652 (2010).
40. Akiyama, K. *et al.* PRIMe: a Web site that assembles tools for metabolomics and transcriptomics. *In Silico Biol.* **8,** 339–345 (2008).
41. Chikayama, E. *et al.* Statistical indices for simultaneous large-scale metabolite detections for a single NMR spectrum. *Anal. Chem.* **82,** 1653–1658 (2010).
42. Schuller, S., Frankel, G. & Phillips, A. D. Interaction of Shiga toxin from *Escherichia coli* with human intestinal epithelial cell lines and explants: Stx2 induces epithelial damage in organ culture. *Cell. Microbiol.* **6,** 289–301 (2004).
43. Gordon, D., Desmarais, C. & Green, P. Automated finishing with Autofinish. *Genome Res.* **11,** 614–625 (2001).
44. Delcher, A. L., Harmon, D., Kasif, S., White, O. & Salzberg, S. L. Improved microbial gene identification with GLIMMER. *Nucleic Acids Res.* **27,** 4636–4641 (1999).
45. Lowe, T. M. & Eddy, S. R. tRNAscan-SE: a program for improved detection of transfer RNA genes in genomic sequence. *Nucleic Acids Res.* **25,** 955–964 (1997).
46. Nakamura, T. *et al.* Cloned cytosine deaminase gene expression of *Bifidobacterium longum* and application to enzyme/pro-drug therapy of hypoxic solid tumors. *Biosci. Biotechnol. Biochem.* **66,** 2362–2366 (2002).
47. Yasui, K. *et al.* Improvement of bacterial transformation efficiency using plasmid artificial modification. *Nucleic Acids Res.* **37,** e3 (2009).

©2011 **Macmillan Publishers Limited. All rights reserved**